MOFs for Phosphane Storage Hot Paper

How to cite:
International Edition: doi.org/10.1002/anie.202217534
German Edition: doi.org/10.1002/ange.202217534

Solid-State Investigation, Storage, and Separation of Pyrophoric PH_3 and P_2H_4 with α-Mg Formate

Anna Widera[+],* *Debora Thöny*[+], *Marcel Aebli, Julius Jacob Oppenheim, Justin L. Andrews, Frederik Eiler, Michael Wörle, Hartmut Schönberg, Norbert Weferling, Mircea Dincă*,* and Hansjörg Grützmacher**

In memory of Professor Marianne Baudler.

Abstract: Phosphane, PH_3—a highly pyrophoric and toxic gas—is frequently contaminated with H_2 and P_2H_4, which makes its handling even more dangerous. The inexpensive metal–organic framework (MOF) magnesium formate, α-[$Mg(O_2CH)_2$], can adsorb up to 10 wt% of PH_3. The PH_3-loaded MOF, PH_3@α-[$Mg(O_2CH)_2$], is a non-pyrophoric, recoverable material that even allows brief handling in air, thereby minimizing the hazards associated with the handling and transport of phosphane. α-[$Mg(O_2CH)_2$] further plays a critical role in purifying PH_3 from H_2 and P_2H_4: at 25°C, H_2 passes through the MOF channels without adsorption, whereas PH_3 adsorbs readily and only slowly desorbs under a flow of inert gas (complete desorption time ≈ 6 h). Diphosphane, P_2H_4, is strongly adsorbed and trapped within the MOF for at least 4 months. P_2H_4@α-[$Mg(O_2CH)_2$] itself is not pyrophoric and is air- and light-stable at room temperature.

Phosphane (PH_3), the simplest phosphorus hydride, is a colorless, pyrophoric, and highly toxic gas.[1,2] Its phosphorus weight content (91.2%) is the highest of all stable commercial phosphorus compounds and its annual industrial production in the US exceeds a couple of thousand tons.[3] Its preparation involves either an acid- or alkali-promoted disproportionation of white phosphorus. It demands harsh reaction conditions and produces acid derivatives such as H_3PO_3 or H_3PO_4, H_2, and diphosphane P_2H_4 as by-products that are difficult to separate.[4,5] PH_3 plays an important role as a doping agent for n-type semiconductors, fumigant, polymerization initiators, and as an intermediate in the preparation of flame retardants.[6–10] Very recently, PH_3 has attracted further interest due to its superconductivity at high pressures and above 100 K.[11–15] PH_3 is also used for the synthesis of primary, secondary, and tertiary phosphanes, H_2PR, HPR_2 and PR_3, which involves addition of phosphorus radicals to hydrocarbons.[16–18] An even broader applicability of PH_3 is, however, hindered by its hazards, which are also caused by impurities from its decomposition to H_2, P_2H_4, and higher phosphanes.[19,20] Previously, Weston et al. investigated phosphane sorption into a series of metal–organic frameworks (MOFs) and proposed transition-metal containing MOFs, namely MOF-74-Co and MOF-74-Mn, as possible candidates for respirator and abatement applications.[10] But, a proof-of-concept study was not performed and specifically the possibility to selectively adsorb PH_3 from gas mixtures with MOFs has not been investigated to our knowledge. In this work, we demonstrate the adsorption/desorption and safe storage of PH_3 in α-Mg formate, an inexpensive, easily produced, environmentally friendly, and commercially available material.[21,22] Our study further provides an updated crystallographic characterization of PH_3, which despite its ubiquity and importance had been previously mischaracterized by X-ray diffraction more than 90 years ago. Finally, we show that α-Mg formate discriminates between PH_3 and its main contaminants H_2, and P_2H_4, and allows trapping and safe handling of pyrophoric P_2H_4 for extended periods under ambient conditions.

We started our investigation by crystallizing PH_3 in a glass capillary at 100 K. The obtained diffraction data obtained with a single crystal reveal a cubic face centered F-

---

[*] Dr. A. Widera,[+] D. Thöny,[+] M. Aebli, F. Eiler, M. Wörle,
H. Schönberg, Prof. H. Grützmacher
Department of Chemistry and Applied Biosciences, ETH Zürich
Vladimir-Prelog-Weg 1–5/10, 8093 Zürich (Switzerland)
E-mail: awidera@inorg.chem.ethz.ch
hgruetzmacher@ethz.ch

J. J. Oppenheim, J. L. Andrews, Prof. Dr. M. Dincă
MIT Department of Chemistry, Massachusetts Institute of Technology
77 Massachusetts Ave., Cambridge, MA-02139 18-393 (USA)
E-mail: mdinca@mit.edu

Dr. N. Weferling
WefConsult GmbH
Knapsackstr. 39, 50354 Huerth (Germany)

[+] These authors contributed equally to this work.

43m space group with a lattice constant of $a = 6.3390(7)$ Å, a cell volume of 254.72(8) Å^3, and four PH_3 molecules per unit cell (Figure 1). This allows us to estimate the effective molecular volume of PH_3 to be 63.7 Å^3. Thereby we correct the only available experimental data obtained by a powder XRD measurement from G. Natta (1930), in which a cubic primitive crystal system with $a = 6.31 \pm 0.01$ Å and a cell volume of 251 Å^3 were assumed.[23]

In contrast to the experimental structure of NH_3 in which every molecule is involved in six hydrogen bonds,[24] for PH_3 only a very weak interaction between the molecules was found. The lack of intramolecular interactions was moreover confirmed in solution by ^{1}H DOSY NMR measurements performed in THF-d_8 and toluene-d_8 (see Supporting Information for details). Solute PH_3 radii of $R_{THF}(PH_3) = 1.248$ Å and $R_{toluene}(PH_3) = 1.150$ Å were found, which are only slightly larger than the reported covalent radius of the P^{III} atom (1.100 Å).[2] From these radii PH_3 solute volumes of 8.1 Å^3 (THF) and 6.4 Å^3 (toluene) were calculated.

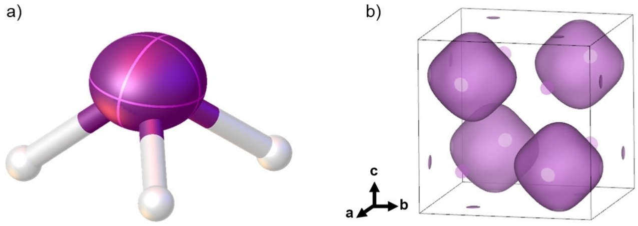

Figure 1. Illustrations of the experimentally determined solid state single crystal structure of PH_3 at 100 K. Thermal ellipsoids are shown at 50% probability level. The structure was solved as rigid group with P–H angles and P–H bond length of 1.421 Å extracted from the literature.[25–27] a) Depiction of one of the possible molecule orientations, b) difference electron density map isosurface given at a level of 0.2 e$^-$ A^{-3} shows no interaction between the PH_3 molecules. For the complete structure see Supporting Information.

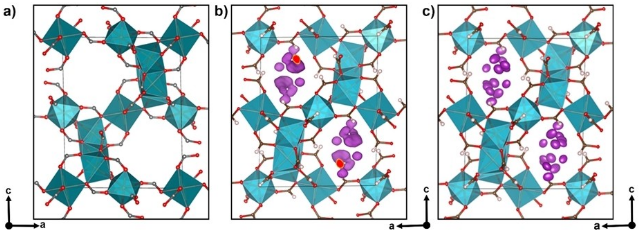

Figure 2. Portions from the experimentally determined single crystal structure of a) the activated α-magnesium formate MOF at 100 K (hydrogen atoms are omitted for clarity) and b) projection of the structure of PH_3@α-$[Mg(O_2CH)_2]$ along the crystallographic b-direction. The residual electron density within the channels after loading is given by an isosurface (purple) at a level of 0.7 e$^-$ A^{-3}. c) Projection of the PH_3@α-$[Mg(O_2CH)_2]$ structure along the crystallographic b-direction. The residual electron density within the channels is described by partially occupied P-atoms (purple), disordered over seven positions. The total occupancy sums up to 0.97(5) P-atoms per asymmetric unit. Thermal ellipsoids are shown at 50% probability level.

Three MOFs were chosen as promising candidates for PH_3 adsorption: (i) Co-MOF-74, $[Co_2(dobdc)]$ (dobdc^{4-} = 2,5-dioxido-1,4-benzenedicarboxylate), (ii) $[Cd_2(ttftb)]$ (ttftb^{4-} = tetrathiafulvalene tetrabenzoate), and (iii) α-magnesium formate, α-$[Mg(O_2CH)_2]$, which is known to reversibly adsorb/desorb ammonia.[28] Unfortunately, the H_2O molecules bound to the metal sites in the single crystals of Co-MOF-74 and $Cd_2(ttftb)$ could not be removed upon heating in vacuum at 120 °C. In these water containing materials, no PH_3 could be introduced. However, the DMF molecules located in the pores of α-$[Mg(O_2CH)_2]$ could be removed by heating to 120 °C for 12 h under dynamic vacuum. The complete loss of DMF with retention of single crystallinity was verified by a structure determination using X-ray diffraction (XRD) methods. The result is shown in Figure 2a. Activated α-$[Mg(O_2CH)_2]$ crystallizes in a **dia** net with 4.5×5.5 Å wide pores[29] with a void size of 128 Å^3, which should be sufficient to host up to 2 molecules of PH_3 ($V_{eff}(PH_3) = 63.7$ Å^3). When evacuated single crystals of α-$[Mg(O_2CH)_2]$ were pressurized under 1.2 bar of PH_3, phosphane was readily adsorbed in the pores. The structure of the PH_3 loaded MOF, PH_3@α-$[Mg(O_2CH)_2]$, was determined by single crystal XRD. The solved structure is shown in Figure 2c.

The cell parameters of pristine α-$[Mg(O_2CH)_2]$ do not change significantly after the loading with PH_3. The Difference Fourier Map of α-$[Mg(O_2CH)_2]$ before loading with PH_3 shows no residual electron density peaks larger than 0.3 e$^-$ A^{-3} within the channels. After loading with PH_3, several significant electron density peaks up to about 3.5 e$^-$ A^{-3} appeared. The corresponding residual electron density isosurface at a 0.7 e$^-$ A^{-3} level is shown in Figure 2b.

For the final refinement, the residual electron density was described by partially occupied P atoms, disordered over seven positions, each of them with anisotropic displacement parameters (cf. Figure 2c). The total occupancy sums up to 0.97(5) P-atoms per asymmetric unit.

Most remarkably, the PH_3-loaded MOF, PH_3@α-$[Mg(O_2CH)_2]$, is not pyrophoric and can even be handled safely in air for short periods. At 30 °C, complete desorption of PH_3 occurs over 6 h, as determined by thermogravimetric analysis (TGA) of PH_3@α-$[Mg(O_2CH)_2]$ under a stream of Ar (see Supporting Information, Figure S37). These findings are in agreement with the calculated preferred binding sites showing multiple possible orientations with a low binding energy of only ca. 2 kcal mol^{-1} (see Supporting Information, Figure S35). The ability of PH_3@α-$[Mg(O_2CH)_2]$ to only slowly release PH_3 allows its utilization as a convenient, safer source of PH_3. Indeed, after suspending PH_3@α-$[Mg(O_2CH)_2]$ crystals in benzene-d_6, phosphane release was observed as indicated by the ^{31}P and ^{1}H NMR spectra of the suspension at room temperature (see Supporting Information, Figure S48–S50). The resulting empty MOF crystals can be recovered by filtration and, after drying under vacuum, they can be reused for subsequent cycles of PH_3 uptake.

Solid-state NMR (SS NMR) provided additional information on the nature of adsorbed phosphane in PH_3@α-[$Mg(O_2CH)_2$]. The ^{1}H NMR spectrum shows two well-defined peaks at $\delta(^1H) = 9.93$ ppm (s, $HCOO^-$) and 3.33 ppm (d, PH_3, $^1J_{PH} = 184$ Hz). The integral ratio of the $HCOO^-$ to PH_3 protons equals 44:3, corresponding to a ratio of one PH_3 molecule per 22 [$Mg(O_2CH)_2$] units. This low PH_3 loading is explained by the relatively long time needed for sample preparation and grinding the crystals, which leads to partial release of phosphane. The $^{31}P\{^1H\}$ solid-state NMR spectrum displays a broad signal, composed of four signals with different integral ratios at $\delta(^{31}P\{^1H\}) = -250.17$ ppm (41 %), -250.37 ppm (7 %), -250.68 ppm (50 %) and -251.02 ppm (2 %) (Figure S29). These signals are assigned to the multiple possible PH_3 orientations inside the MOF channel, as also observed in the solid-state structure (cf. Figure 2). Interestingly, the $^{31}P\{^1H\}$ integrated peak intensities of the PH_3 species change over time (Figure S31): After 48 h the signal at $\delta(^{31}P\{^1H\}) = -250.17$ ppm disappears and the signal at $\delta(^{31}P\{^1H\}) = -250.72$ ppm represents the major orientation (73 %) of PH_3 molecules in the MOF, followed by the signals at $\delta(^{31}P\{^1H\}) = -250.38$ ppm (23 %) and $\delta(^{31}P\{^1H\}) = -251.11$ ppm (4 %) (Figure S31) indicating that PH_3 molecules reorient in the MOF with time. Only 8 % of the initial PH_3 molecules leaked from the rotor under the conditions of the ^{31}P MAS NMR experiment at 25 °C (Figure S33). At low temperature (95 K), a broad asymmetric $^{31}P\{^1H\}$ signal at $\delta = -251.00$ ppm is observed (Figure S41), which—after warming to room temperature—changes shape demonstrating the dynamic behavior of PH_3 molecules and reordering processes inside the MOF with increasing temperature. The interaction of the adsorbed PH_3 with the formate anions in the MOF is evident as a cross peak in the ^{1}H-^{31}P cpHETCOR NMR spectrum (Figure S39). Furthermore, a cross peak between the PH_3 protons and a signal of an impurity at $\delta(^{31}P) = -217.00$ ppm is visible. Commercially available PH_3 is contaminated with P_2H_4, and we assign this coupling to an interaction of PH_3 with P_2H_4 likewise adsorbed inside the MOF {Lit.: $\delta(^{31}P(P_2H_4)) = -204.97$ ppm}.[30] To investigate possible P_2H_4 adsorption in more detail and to ascertain whether there is a certain degree of selectivity with respect to the adsorption of PH_3, H_2, and P_2H_4—the two latter are the most important by-products in commercial phosphane production—we carried out three experiments. First, single crystals of activated α-[$Mg(O_2CH)_2$] were pressurized with H_2. No H_2 uptake could be observed at room temperature, in line with previous reports.[31] Next, we attempted to load diphosphane by suspending activated MOF single crystals in freshly prepared P_2H_4.[32,33] The single crystals were subsequently collected and subjected to XRD analysis. The resulting structure is shown in Figure 3a,b. Molecules of P_2H_4 are observed in 2 possible positions (with occupancy factors of 70 % and 19 %, respectively) inside the MOF, aligned in zigzag fashion along each channel (Figure 3b).

We could not localize the hydrogen atoms of P_2H_4 due to disorder. However, we were able to refine P–P distances of 2.16 Å and 2.21 Å, which are in good agreement with an expected P–P single bond length of 2.20 Å.[2]

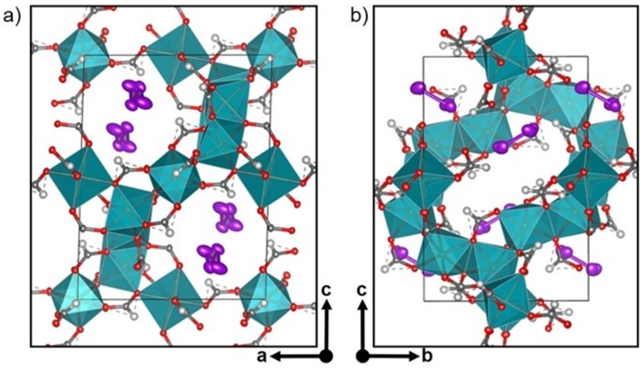

Figure 3. Portions from the experimentally determined single crystal structure of the P_2H_4 loaded α-magnesium formate MOF at 100 K from two perspectives, a) along the crystallographic b-direction and b) along the crystallographic a-direction. The positions of the phosphorus bound hydrogen atoms are not determined. Thermal ellipsoids are shown at 50 % probability level. Selected bond lengths [Å]: P1–P2 2.206(3), P3–P4 2.159(17).

In contrast to free diphosphane, which is highly pyrophoric, P_2H_4 adsorbed into the channels of α-[$Mg(O_2CH)_2$] shows excellent stability. P_2H_4@α-[$Mg(O_2CH)_2$] is a non-pyrophoric, air-, room temperature-, and UV/Vis-light-stable substance which can be kept in open air over several weeks. This betrays tight adsorption of P_2H_4 molecules, which remain inside the MOF even after 4 months of storage in air, with no sign of oxidation, as verified via single crystal XRD (26 % (anisotropically refined) and 4 % (isotropically refined) occupancy, Figure S51). In contrast to PH_3, P_2H_4 is not released from the MOF even when suspended in an organic solvent such as benzene. Its release is only possible upon dissolving P_2H_4@α-[$Mg(O_2CH)_2$] crystals in degassed water. During this process, P_2H_4 is degraded mainly to phosphorous acid, H_3PO_3, although a significant amount of P_2H_4 is still present in the solution after 6 h (Figure S52). The different PH_3 and P_2H_4 affinities of the MOF were confirmed by density functional theory at the PBE/DND level of theory. Whereas adsorbed PH_3 is favorable by $\Delta E(PH_3) = -4.69\ \mathrm{kcal\,mol^{-1}}$ relative to free PH_3 in the gas phase, MOF-bound P_2H_4 is even more stable than the free P_2H_4 with $\Delta E(P_2H_4) = -6.70\ \mathrm{kcal\,mol^{-1}}$ (Figure S55).

To determine the discriminating ability of α-[$Mg(O_2CH)_2$] towards the two phosphorus species, we subjected crystals of the MOF to a PH_3:P_2H_4 (5:3) mixture, obtained serendipitously by hydrolysis of Ca_3P_2 according to a procedure published by Baudler et al.[32] A ^{31}P SS NMR spectrum of the loaded solid showed two broad non-symmetric signals at $\delta(^{31}P) = -215.18$ ppm (P_2H_4) and $\delta(^{31}P) = -249.00$ ppm (PH_3) (Figure S53). In agreement with the rather fast release of PH_3, we found a decrease of the PH_3 signal integral over time while the integrated signal intensity for P_2H_4 remained constant (Figure S54). After 90 h at room temperature, the integrated signal ratio of PH_3:P_2H_4 was 0.7, corresponding to a PH_3:P_2H_4 molar composition of 4:3. Treating the sample under vacuum for additional 27 h at room temperature only very slightly diminished this ratio to 0.68. These findings are at first glance surprising since the

PH_3 desorption time amounts to 6 h. However, the co-adsorbed larger diphosphane molecules remain encapsulated in the MOF under these conditions and likely block exit channels for the smaller PH_3 molecules, which are therefore entrapped, a phenomenon often observed in filters.

The initially $PH_3:P_2H_4$ (4:3) filled MOF was investigated by TGA after 10 weeks of aging under inert gas. A constant mass decay starting from 40 °C to 185 °C was observed (Figure S56). In the TGA-coupled mass spectrometer a m/z signal of 34 $g\,mol^{-1}$ was found, confirming the PH_3 desorption. Mass spectrometry did not reveal any evidence for free P_2H_4, most likely due to its increasing thermal instability above 40 °C. Likewise, a ^{31}P SS NMR spectrum of the heated MOF did not show any signals of PH_3, P_2H_4 or polyphosphine (Figure S57). These results motivate further investigations of α-[$Mg(O_2CH)_2$] for purification and stabilization of other highly reactive gaseous molecules.

Despite its apparent ubiquity and critical role in several industries, the synthetic potential of PH_3 is still very much underexplored due to its toxicity and pyrophoric nature. The inexpensive and environmentally friendly magnesium formate, α-[$Mg(O_2CH)_2$], lowers this risk to a minimum by adsorbing up to 10 wt % PH_3 into its channels. The phosphane-loaded MOF can be stored and even briefly handled in air without ignition. When needed in a reaction, harmless, solid PH_3@α-[$Mg(O_2CH)_2$] can be suspended in an organic solvent whereby PH_3 is released. This study may encourage the search for MOFs with an even higher phosphane affinity, which would allow storing of PH_3 for even longer times. This work also shows in a preliminary fashion that MOFs may become suitable filters in order to clean PH_3 from H_2 and P_2H_4. While hydrogen directly passes through the MOF channels, PH_3 remains temporarily adsorbed, and diphosphane is trapped inside the MOF for at least 4 months. Relatedly, the strong adsorption of diphosphane enables the use of α-[$Mg(O_2CH)_2$] as a safe long-term P_2H_4 trapping or storage material which can be handled in air.

Acknowledgements

Dr. Anna Widera gratefully acknowledges the financial support by the Walter Benjamin program (project nr. 458684978) of the German Research Foundation (DFG). We thank ETH Zürich (ETH-46 21-1) and Louis Kang (PhoSmart Holdings Limited) for additional financial support. Work in the Dincaˇ laboratory at MIT was supported by the US National Science Foundation (DMR-2105495). Open Access funding provided by Eidgenössische Technische Hochschule Zürich.

Conflict of Interest

The authors declare no competing interests.

Data Availability Statement

The data that support the findings of this study are available in the Supporting Information of this article.

Keywords: Gas Purification · Gas Storage · MOF Chemistry · Phosphane · Single Crystal Analysis

---

[1] T. M. Hood, S. Lau, R. L. Webster, *J. Am. Chem. Soc.* **2022**, *144*, 16684–16697.
[2] A. F. Hollemann, E. Wiberg, N. Wiberg, *Anorganische Chemie*, 103th ed., De Gruyter, Berlin, **2017**.
[3] United States Environmental Protection Agency, 1990b. U.S. Environmental Protection Agency, Computer Printout (TSCAPP): 1977 Production Statistics for Chemicals in the Nonconfidential Initial TSCA Chemical Substances Inventory. Washington, DC: Office of Pesticides and Toxic Substances.
[4] D. J. Scott, J. Cammarata, M. Schimpf, R. Wolf, *Nat. Chem.* **2021**, *13*, 458–464.
[5] G. Bettermann, W. Krause, G. Riess, T. Hofmann, *Inorganic Phosphorus Compounds in Ullmann's Encyclopedia of Industrial Chemistry*, Wiley-VCH, Weinheim, **2000**.
[6] L. Li, T. Liu, B. Li, F. Zhang, S. Dong, Y. Wang, *J. Econ. Entomol.* **2014**, *107*, 601–605.
[7] M. A. Chaudhry, *Pestic. Sci.* **1997**, *49*, 213–228.
[8] Y. Wang, K.-K. Lew, T.-T. Ho, L. Pan, S. W. Novak, E. C. Dickey, J. M. Redwing, T. S. Mayer, *Nano Lett.* **2005**, *5*, 2139–2143.
[9] Y. Yamamoto, J. Murota, B. Tillack, *ECS Trans.* **2010**, *33*, 995.
[10] M. H. Weston, W. Morris, P. W. Siu, W. J. Hoover, D. Cho, R. K. Richardson, O. K. Farha, *Inorg. Chem.* **2015**, *54*, 8162–8164.
[11] H. Liu, Y. Li, G. Gao, J. S. Tse, I. I. Naumov, *J. Phys. Chem. C* **2016**, *120*, 3458–3461.
[12] A. Shamp, T. Terpstra, T. Bi, Z. Falls, P. Avery, E. Zurek, *J. Am. Chem. Soc.* **2016**, *138*, 1884–1892.
[13] T. Bi, D. P. Miller, A. Shamp, E. Zurek, *Angew. Chem. Int. Ed.* **2017**, *56*, 10192–10195; *Angew. Chem.* **2017**, *129*, 10326–10329.
[14] A. P. Durajski, *Sci. Rep.* **2016**, *6*, 38570.
[15] A. P. Drozdov, M. I. Eremets, I. A. Troyan, Preprint at https://arxiv.org/abs/1508.06224.
[16] J. Svara, N. Weferling, T. Hofmann, *Organic Phosphorus Compounds in Ullmann's Encyclopedia of Industrial Chemistry*, Wiley-VCH, Weinheim, **2006**.
[17] A. R. Stiles, F. F. Rust, W. E. Vaughan, *J. Am. Chem. Soc.* **1952**, *74*, 3282–3284.
[18] M. M. Rauhut, H. A. Currier, A. M. Semsel, V. P. Wystrach, *J. Org. Chem.* **1961**, *26*, 5138–5145.
[19] Y. Yuan, Y. Li, G. Fang, G. Liu, C. Pei, X. Li, H. Zheng, K. Yang, L. Wang, *Natl. Sci. Rev.* **2019**, *6*, 524–531.
[20] M. Liu, X. Huang, X. Wang, Y. Huang, F. Li, G. Wu, X. Li, Y. Liang, D. Zhou, M. Lu, B. Liu, T. Cui, *J. Raman Spectrosc.* **2018**, *49*, 721–727.
[21] J. Xu, V. V. Terskikh, Y. Huang, *Chem. Eur. J.* **2013**, *19*, 4432–4436.
[22] T. Hussain, P. Nie, B. Hu, X. Shang, J. Yang, J. Liu, *J. Mater. Sci.* **2021**, *56*, 10282–10292.
[23] G. Natta, E. Casazza, *Gazz. Chim. Ital.* **1930**, *60*, 851–859.
[24] R. Boese, N. Niederprüm, D. Bläser, A. Maulitz, M. Yu. Antipin, P. R. Mallinson, *J. Phys. Chem. B* **1997**, *101*, 5794–5799.
[25] D. Corbridge, *Phosphorus: Chemistry, Biochemistry and Technology*, 6th ed., Taylor & Francis, New York, **2013**.
[26] A. V. G. Chizmeshya, C. Ritter, J. Tolle, C. Cook, J. Menéndez, J. Kouvetakis, *Chem. Mater.* **2006**, *18*, 6266–6277.

[27] M. Ceppatelli, D. Scelta, M. Serrano-Ruiz, K. Dziubek, G. Garbarino, J. Jacobs, M. Mezouar, R. Bini, M. Peruzzini, *Nat. Commun.* **2020**, *11*, 6125.
[28] I. Spanopoulos, I. Bratsos, C. Tampaxis, A. Kourtellaris, A. Tasiopoulos, G. Charalambopoulou, T. A. Steriotis, P. N. Trikalitis, *CrystEngComm* **2015**, *17*, 532–539.
[29] H. Mao, J. Xu, Y. Hu, Y. Huang, Y. Song, *J. Mater. Chem. A* **2015**, *3*, 11976–11984.
[30] P. Junkes, M. Baudler, J. Dobbers, D. Rackwitz, *Z. Naturforsch. B* **1972**, *27*, 1451–1456.
[31] B. Schmitz, I. Krkljus, E. Leung, H. W. Höffken, U. Müller, M. A. Hirscher, *ChemSusChem* **2010**, *3*, 758–761.
[32] M. Baudler, H. Ständeke, M. Borgardt, H. Strabel, J. Dobbers, H. Muntenbeck, C. P. Schöner, W. Faber, U. M. Krause, W. Kronenberg, *Z. Anorg. Allg. Chem.* **1995**, *621*, 1133–1139.
[33] Gmelin, *Handbook of Inorganic and Organometallic Chemistry*, Phosphorus Suppl. Vol. C2, 8th ed., Springer Verlag Berlin and Heidelberg, Berlin, **1996**, pp. 16–17.

Manuscript received: November 28, 2022
Accepted manuscript online: January 16, 2023
Version of record online: ■■, ■■

Communications

MOFs for Phosphane Storage

A. Widera,* D. Thöny, M. Aebli,
J. J. Oppenheim, J. L. Andrews, F. Eiler,
M. Wörle, H. Schönberg, N. Weferling,
M. Dincaˇ,*
H. Grützmacher* ________ **e202217534**

Solid-State Investigation, Storage, and Separation of Pyrophoric PH_3 and P_2H_4 with α-Mg Formate

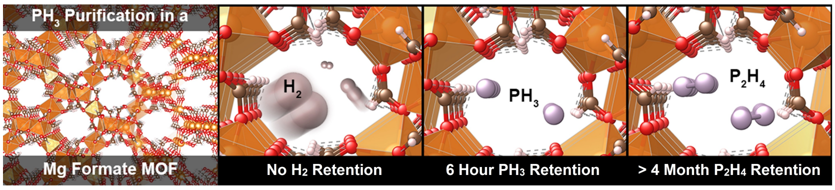

Phosphane, PH_3, is a highly pyrophoric and toxic gas that is often contaminated with H_2 and P_2H_4. The inexpensive α-Mg formate MOF adsorbs up to 10 wt% of PH_3 and allows safe handling of phosphane in air. This MOF is moreover a candidate for PH_3 purification and long-time P_2H_4 storage in air and at room temperature.